Hierarchical porous amorphous metal-organic frameworks constructed from ZnO/MOF glass composites

Ying Feng,[a,b] Jia-Xuan Wu,[a] Yi-Hong Mo,[a] Shuai Liu,[a] Song-Liang Cai,[a] Wei-Guang Zhang,[a]* Jun Fan,[a]* Sheng-Run Zheng[a]*

[a]GDMPA Key Laboratory for Process Control and Quality Evaluation of Chiral Pharmaceuticals, and Guangzhou Key Laboratory of Analytical Chemistry for Biomedicine, School of Chemistry, South China Normal University, Guangzhou 510006, China
[b]School of Chemistry, Guangdong University of Petrochemical Technology, Maoming 525000, China

* Corresponding author: Prof. Sheng-Run, Zheng; Prof. Jun Fan; Prof. Wei-Guang Zhang

E-mail address: zhengsr@scnu.edu.cn; fanj@scnu.edu.cn; wgzhang@scnu.edu.cn

Tel./Fax. : +86-20-39310187

Supporting Information

EXPERIMENTAL SECTION

Materials and Measurements

Imidazole and 5-chlorobenzimidazole were of analytical grade and were purchased from Shanghai Aladdin Biochemical Technology Co., Ltd. The other chemicals were of analytical grade and were purchased from Guangzhou Chemical Reagent Factory. Fourier transform infrared (FTIR) spectra (Platinum Elmer Spectrum) were measured with the KBr pressed-disc method in the range of 4000 to 400 cm^{-1}. Powder X-ray diffraction (PXRD) data were collected using Cu Kα radiation (k = 1.5406 Å) at 40 kV and 40 mA at room temperature on an Ultima IV X-ray powder diffractometer. Thermogravimetric analysis (TGA) curves were obtained on a NETZSCH STA-409PC system heated from room temperature to 800 °C at a heating rate of 10 °C/min under air. X-ray photoelectron spectroscopy (XPS) data were recorded on a Shimadzu AXIS

SUPRA X-ray photoelectron spectrometer. Inductively coupled plasma (ICP) data were obtained on a Pastor Spectro Arcos MV Plasma Emission Spectrometer. SEM images were recorded on a German ZEISS Ultra 55 field emission scanning electron microscope.

Synthesis of ZnO/agZIF-76 composites

ZIF-76 crystals and agZIF-76 were synthesized according to the literature.[1] To synthesize the composites, first, nano-ZnO (a mg), ZIF-76 crystals (100 mg), 1-n-butylamine (100 μL), and ethanol (10 mL) were added to a ball milling tank. The mixture was ground by ball milling at 400 rpm for 15 minutes to obtain a mixture of ZnO and ZIF-76. Second, the mixtures were prepressed into circular flakes under a pressure of 10 MPa and then heated at 470 ℃ for 1 hour (at a 10 ℃ min-1 heating rate from room temperature) under an argon atmosphere (flow rate set at 5 $ml \cdot min^{-1}$). Finally, the sample was quenched at 10 $℃ \cdot min^{-1}$ to room temperature, and the products were washed with anhydrous ethanol and dried to obtain composites of agZIF-76 and ZnO, with yields higher than 90%. The samples were denoted as ZnO/agZIF-76-x (where x = 10%, 20%, 40%, and 60%, representing the mass fraction of ZnO in the composite material).

Synthesis of aZIF-76

The ZnO/agZIF-76-x (30 mg) samples were immersed in ammonia solution for 2 days. Then, the resulting products were filtered, washed with deionized water, and dried at 100 ℃ for 12 hours under vacuum. The obtained products were denoted as HP-aZIF-76-x-y (y = 5%, 15%, and 25%, representing the mass concentrations of the ammonia solution). The yield of HP-aZIF-76-x-y ranged from 60% to 90%.

EXAFX analysis

Data reduction, data analysis, and EXAFS fitting were performed and analysed with the Athena and Artemis programs of the Demeter data analysis packages[2], which utilize the FEFF6 program[3] to fit the EXAFS data. The energy calibration of the sample was conducted through a standard Zn foil, which was simultaneously measured as a reference. A linear function was subtracted from the preedge region, and the edge jump was subsequently normalized using Athena software. The χ(k) data were isolated by subtracting a smooth, three-stage polynomial approximating the absorption background of an isolated atom. The k3-weighted χ(k) data were Fourier transformed after applying a Hanning window function (Δk = 1.0). For EXAFS modelling, the global amplitude EXAFS (*CN, R,* σ^2 and ΔE_0) was obtained by nonlinear fitting, with least-squares

refinement, of the EXAFS equation to the Fourier transformed data in R-space. Using Artemis software, the EXAFS of the Zn foil was fitted, and the obtained amplitude reduction factor S_0^2 value (0.802) was set in the EXAFS analysis to determine the coordination numbers (CNs) in the Zn-N/O/Zn scattering path in the sample.

Gas adsorption measurements

Gas adsorption–desorption isotherms were measured on a BSD-660 M A6M Physical Adsorption Analyser. The temperature was maintained at 77 K by using a liquid nitrogen bath and at other specified temperatures by using a chiller (Dewar) with a circulating jacket connected to a thermostatic bath. Ultrahigh-purity N_2 (99.9999%), Ar (99.9999%), C_2H_2 (99.9%), C_2H_4 (99.5%), C_2H_6 (99.5%), CO_2 (99.999%), and CH_4 (99.99%) were used for all the adsorption measurements. Prior to the adsorption measurements, the samples were degassed using a high vacuum pump (μm Hg) at 373 K for more than 12 h.

Breakthrough experiment

The breakthrough experiments were carried out in a homemade apparatus. The sample was dried under vacuum at 100 °C for 12 h. Samples (approximately 200 mg) were then introduced to the adsorption bed (φ3 mm × 60 mm). A carrier gas (He ≥99.999%) was used to purge the adsorption bed for more than 1 h to ensure that the adsorption bed was saturated with He. Then, the gas flow was switched to the desired gas mixture without any inert gas dilution (CH_4/C_2H_2 = 90/10) at a flow rate of 20 mL/min. The recovery gas was passed to an analyser port and analysed using a quantitative gas analysis mass spectrometer (DECRA HIDEN) with a thermal conductivity detector (TCD).

rediction of the Gas Adsorption Selectivity by IAST.

The ideal adsorbed solution theory (IAST) was used to predict the adsorption selectivity from the experimental pure gas isotherms. First, the adsorption isotherms of the selected gas were fitted by the Langmuir-Freundlich (1) model to allow the application of IAST in simulating the performance of the samples under mixed component gas.

$$N = \frac{A_1 b_1 p^{c1}}{1 + b1\, p^{c1}} \quad \text{..... (1)}$$

Here, p is the pressure of the bulk gas at equilibrium with the adsorbed phase (bar), N is the molar loading of the adsorbate (mmol/g), A_1 is the saturation or maximum loading (mmol/g), b is the affinity coefficient (bar^{-1}) and $c1$ is the adsorbate-adsorbent

interaction (surface heterogeneity) parameter. We employed the fitting parameter for the prediction of multicomponent adsorption with IAST. The adsorption selectivities, $S_{1/2}$, in a binary mixture are represented as $(x_1/x_2)/(y_1/y_2)$, where x_i is the molar fraction of species i in the adsorbed phase and y_i is the molar fraction of species i in the bulk phase.

$$S_{1/2} = \left(\frac{x_1}{x_2}\right)\left(\frac{y_2}{y_1}\right) \quad \text{..... (2)}$$

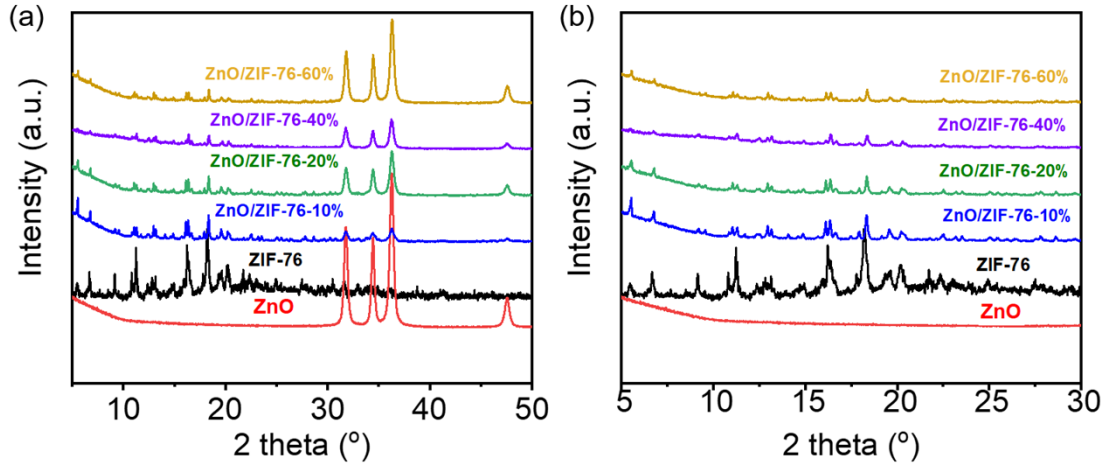

Fig. S1 PXRD patterns of ZnO, ZIF-76 and mixtures of ZnO and ZIF-76 with different mass ratios in the ranges of (a) 5 to 50° and (b) 5 to 30°.

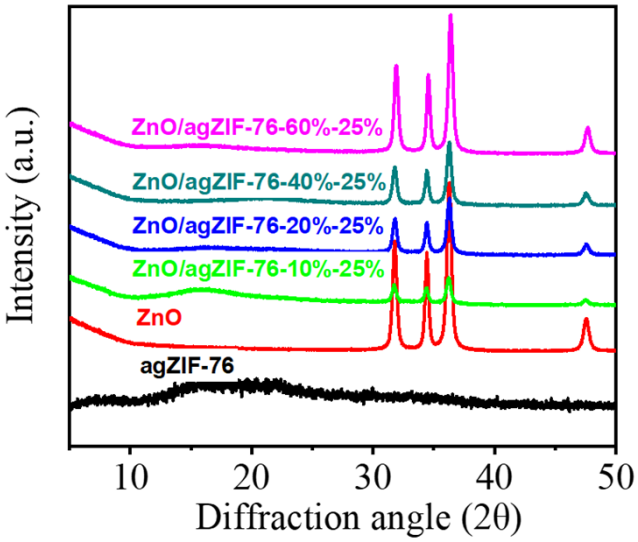

Fig. S2 The PXRD of ZnO, agZIF-76, and ZnO/agZIF-76-x-25% (x = 10, 20, 40, and 60%).

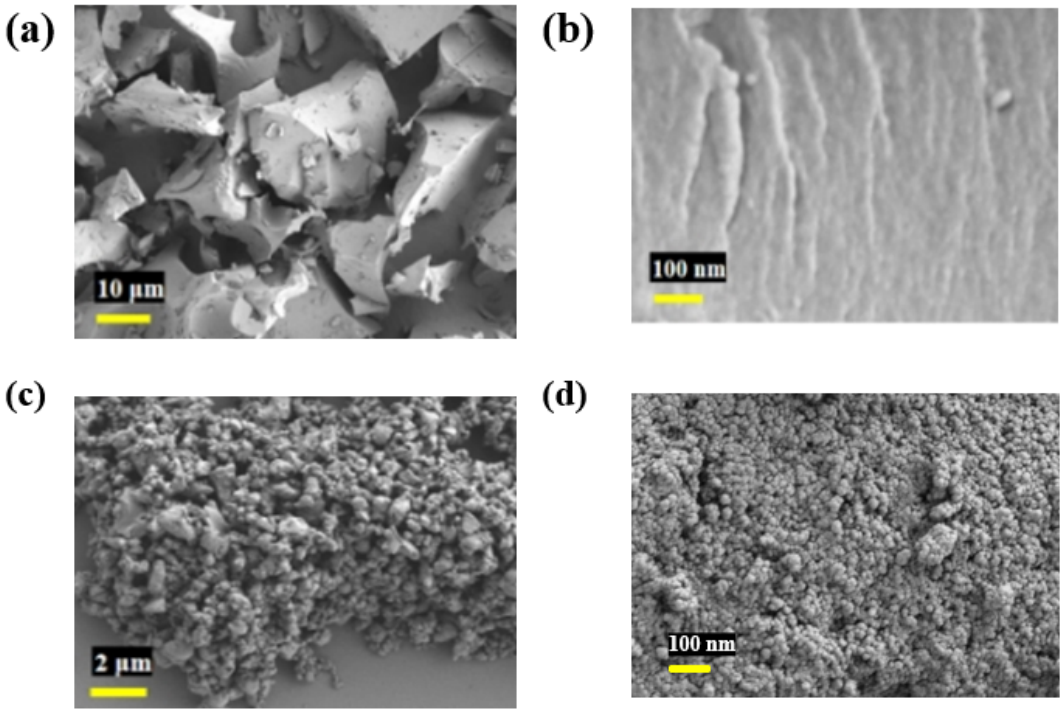

Fig. S3 SEM of (a, b) ZnO/agZIF-76-40% and (c, d) aZIF-76-40%-25%.

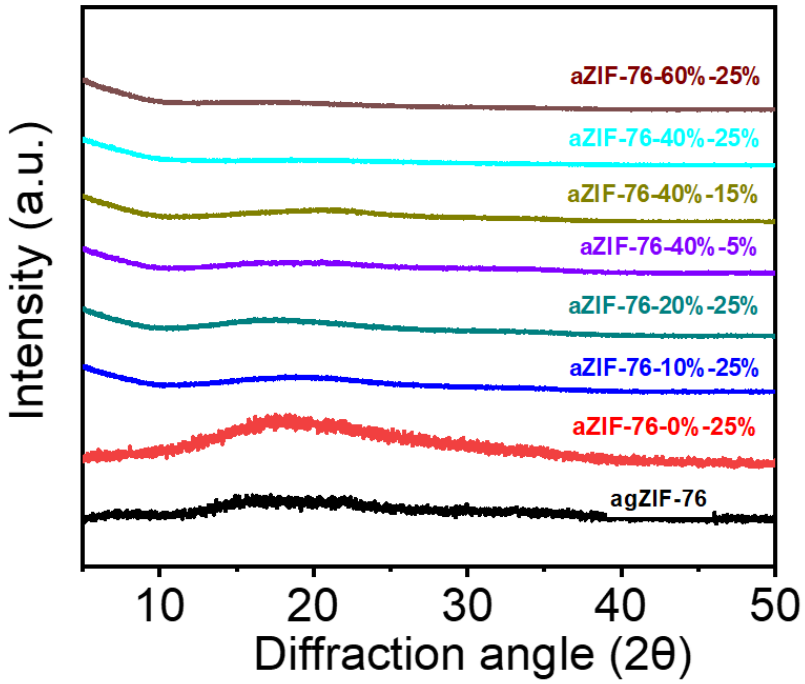

Fig. S4 The PARD of agZIF-76, and serials of aZIF-76.

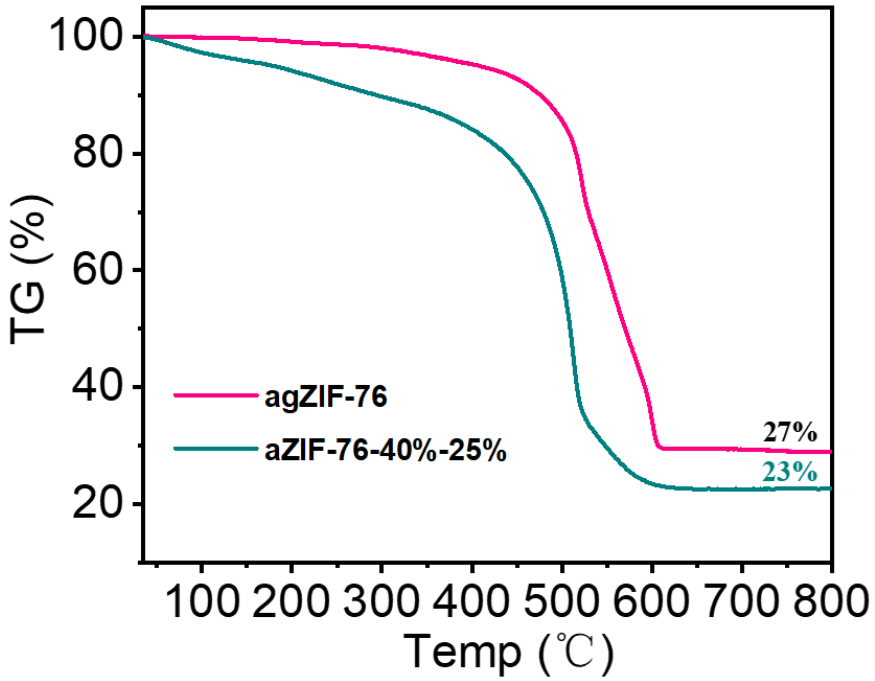

Fig. S5 The TG curve of agZIF-76 and aZIF-76-40%-25%.

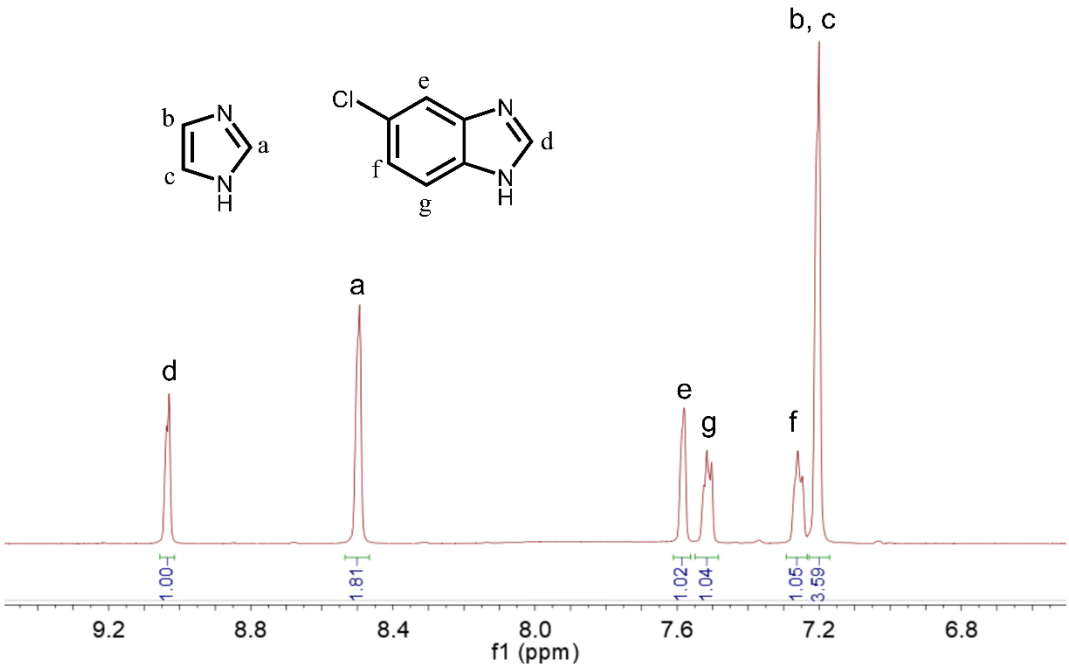

Fig. S6 ^{1}HNMR spectrum of agZIF-76 digested by in DCl/DMSO-d_6.

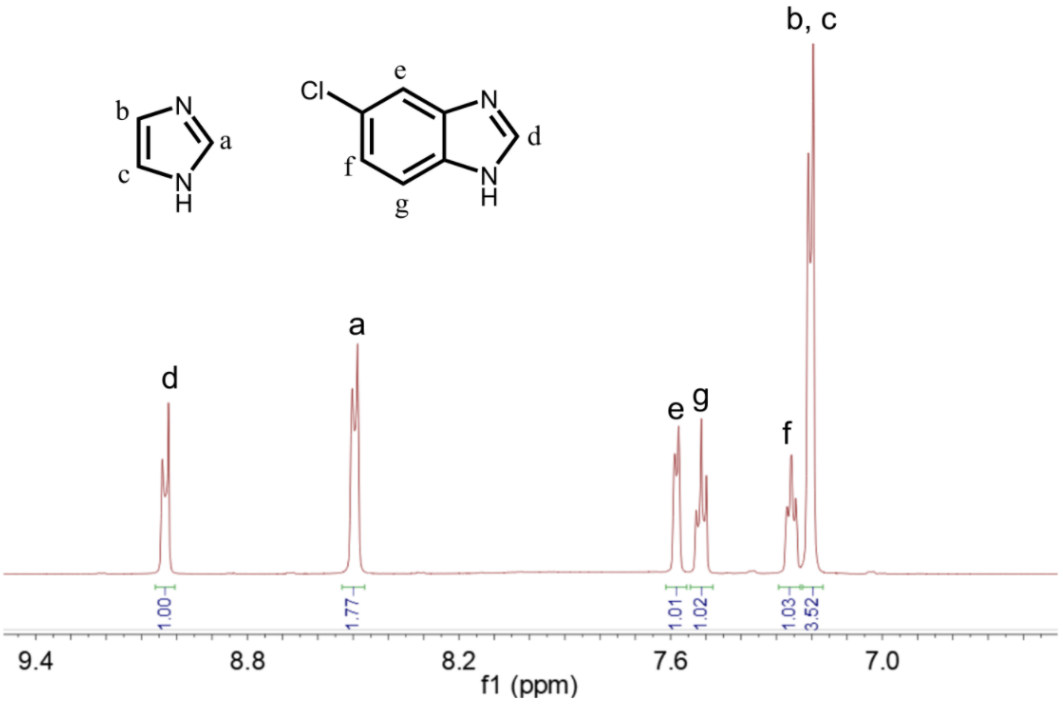

Fig. S7 [1]HNMR spectrum of agZIF-76-40%-25% digested by in DCl/DMSO-d_6.

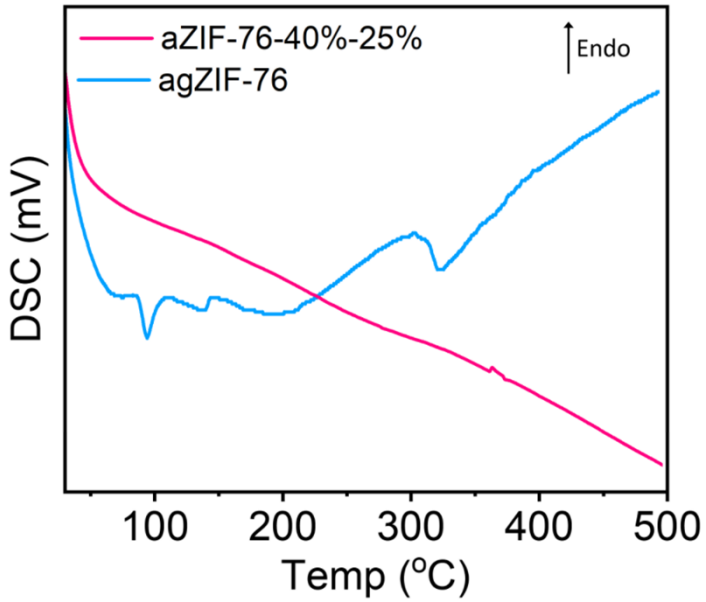

Fig. S8 DSC curve of agZIF-76 and aZIF-76-40%-25%.

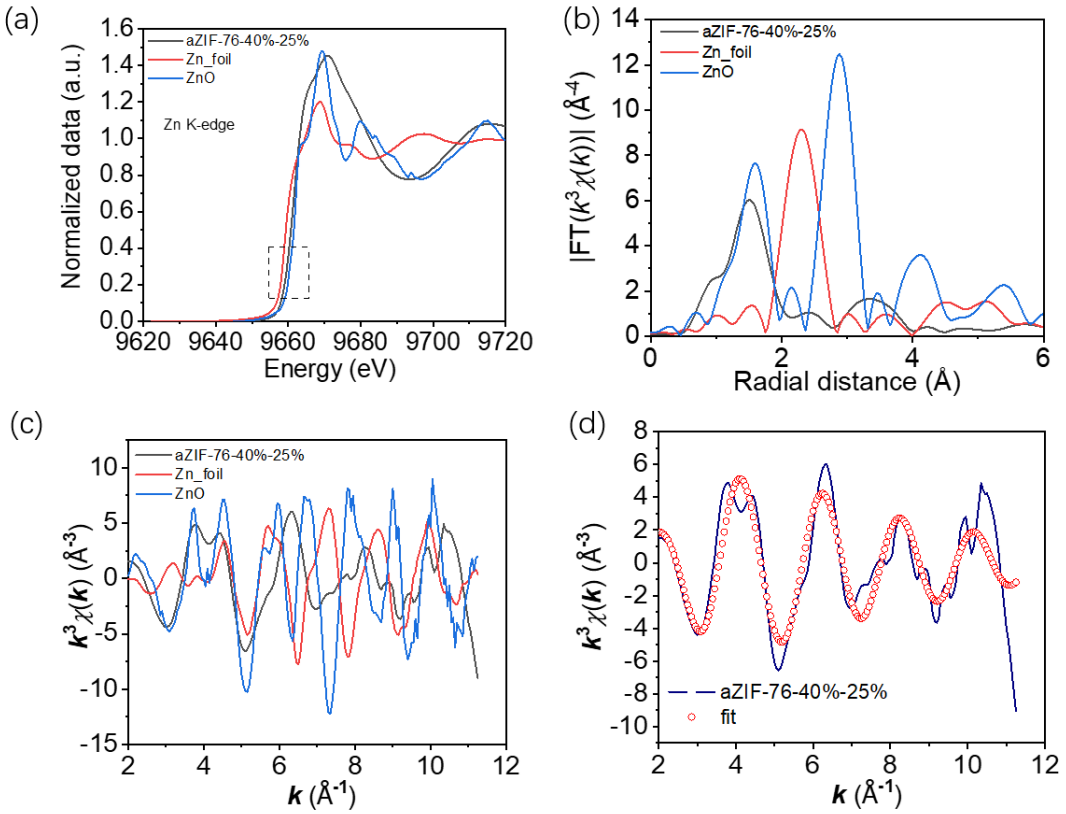

Fig. S9 (a) K-edge XANES spectra of aZIF-76-40%-25% and reference samples of ZnO and Zn foil. Fourier transform extended X-ray absorption structure spectra at the Co K-edge of aZIF-76-40%-25%, reference samples of ZnO and Zn foil at the (b) R(f) and (c) K(e) spaces. (d) EXAFS fitting results of the FT-EXAFX spectra at the Zn K-edge of aZIF-76-40%-25% at the K(e) spaces.

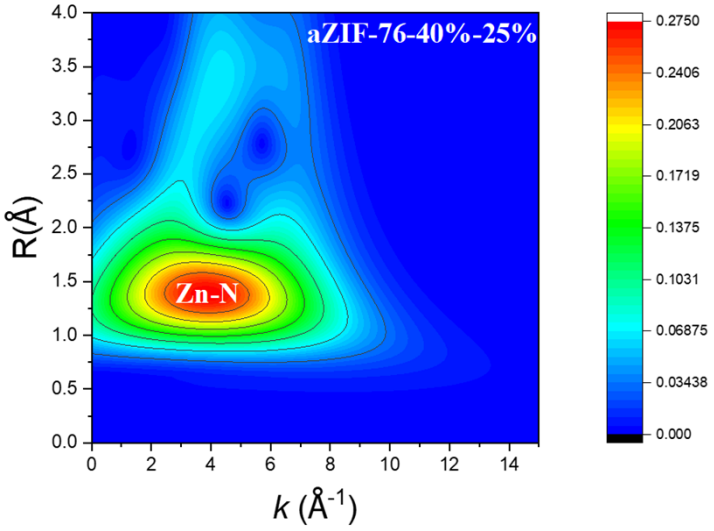

Fig. S10 The Morlet wavelet transform of calculated EXAFS signals for aZIF-76-40%-25%. κ = 5 and σ = 1.

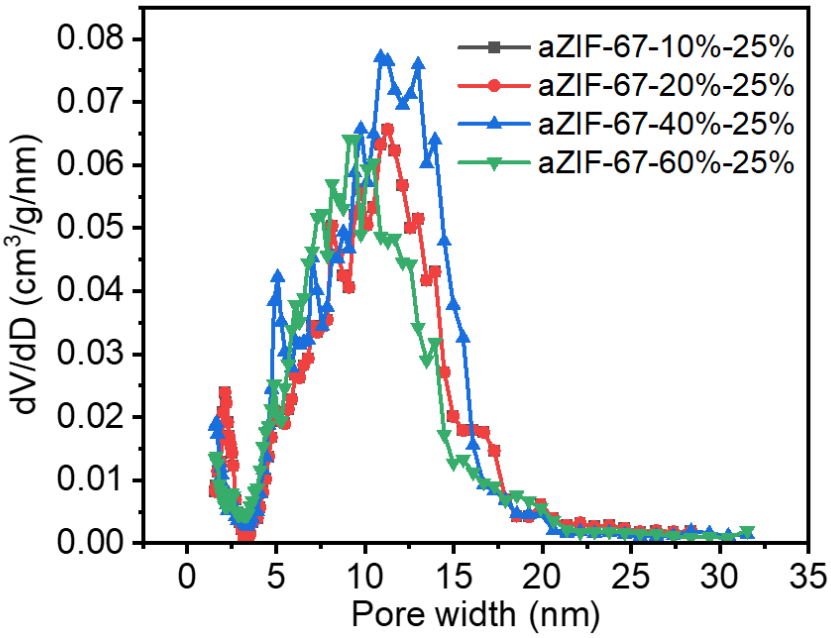

Fig. S11 Pore size distributions obtained from NLDFT mode for aZIF-76-x-25% (x = 10, 20, 40 and 60%) at 77 K.

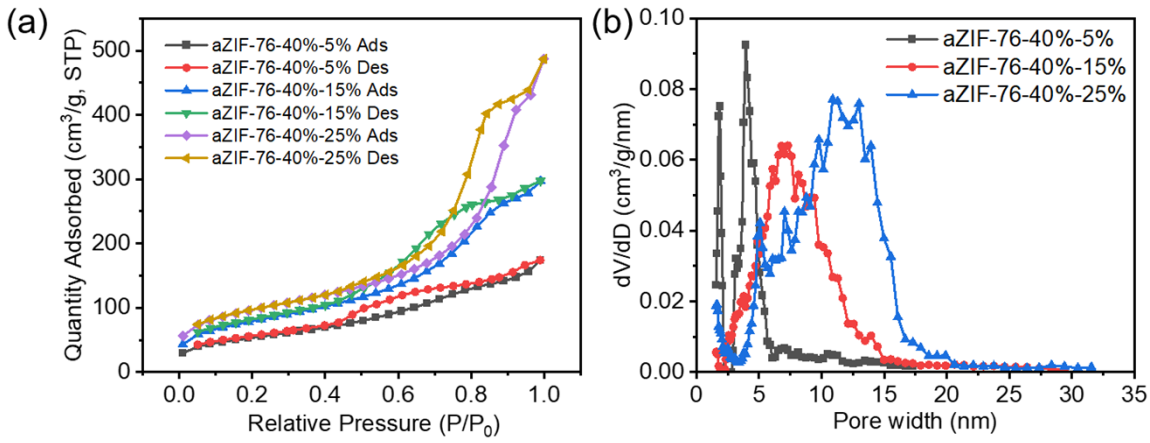

Fig. S12 (a) N_2 adsorption-desorption isotherms and (b) pore size distributions for aZIF-76-40%-y (y = 5, 15, and 25%) at 77 K.

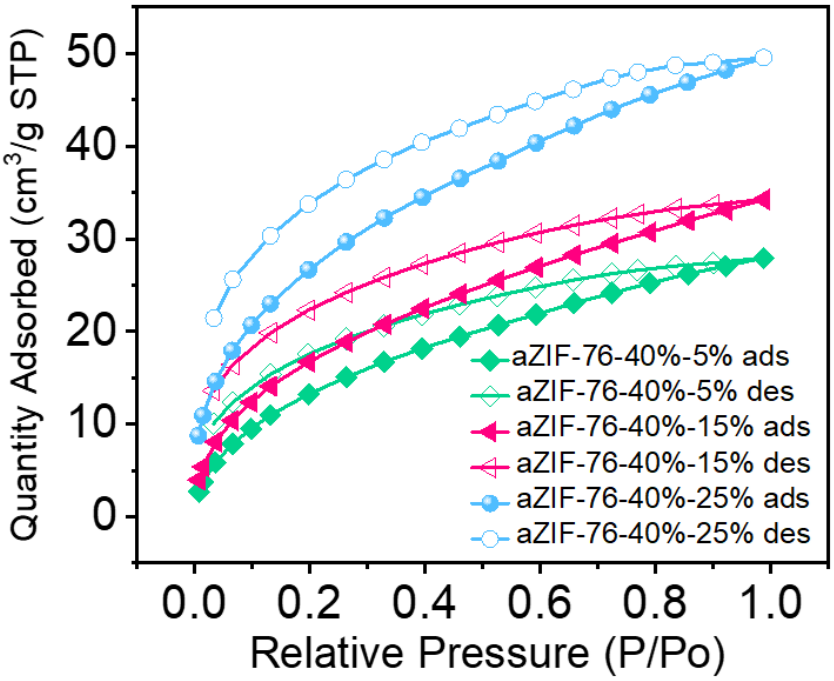

Fig. S13 The CO_2 adsorption-desorption isotherms for aZIF-76-40%-y (y = 5, 15, and 25%) at 273 K.

Table S1. EXAFS fitting parameters at the Zn *K*-edge for various samples.

Sample	Shell	*CN*[a]	*R*(Å)[b]	σ^2(Å^2)[c]	ΔE_0(eV)[d]	*R* factor
Zn foil	Zn-Zn	12*	2.641±0.009	0.0114	-0.6	0.0055
ZnO	Zn-O	4.0±0.2	1.974±0.013	0.0049	4.7	0.0075
	Zn-O-Zn	12.1±0.3	3.222±0.022	0.0090	2.2	
aZIF-76-40%-25%	Zn-N	3.8±0.4	1.966±0.021	0.0061	3.9	0.0076

[a]*CN*, coordination number; [b]*R*, the distance to the neighboring atom; [c]σ^2, the mean square relative displacement (MSRD); [d]ΔE_0, inner potential correction; the *R* factor indicates the goodness of fit. $S0^2$ was fixed to 0.983, according to the experimental EXAFS fit of Zn foil by fixing *CN* as the known crystallographic value. *This value was fixed during EXAFS fitting, based on the known structure of Zn. Fitting range: $3.0 \le k$ (Å) ≤ 11.0 and $1.0 \le R$ (Å) ≤ 3.0 (Zn foil); $3.0 \le k$ (Å) ≤ 11.5 and $1.0 \le R$ (Å) ≤ 3.5 (ZnO); $3.0 \le k$ (Å) ≤ 10.0 and $1.0 \le R$ (Å) ≤ 2.2 (911-1Zn). The EXAFS fitting parameters were as follows: $0.700 < S_0^2 < 1.000$; $CN > 0$; $\sigma^2 > 0$ Å^2; $|\Delta E_0| < 15$ eV; and *R* factor < 0.02.

Table S2 Mesopore porosity analysis for aZIF-76-x-25%.

Sample	[a]S_{BET} (m^2/g)	[b]V_{meso}/[c]V_{micro}	[d]D_{NLDFT} (nm)
aZIF-76-10%-25%	265.53	0.98	1.5~19.9
aZIF-76-20%-25%	290.33	1.02	1.5~19.9
aZIF-76-40%-25%	338.28	0.97	1.5~19.9
aZIF-76-60%-25%	297.75	0.98	1.5~19.9

Table S3 Micropore porosity analysis for aZIF-76-x-25%.

Samples	[a]S_{BET} (m^2/g)	[b]V_{micro} (cm^3/g)	[c]D_{NLDFT} (nm)
aZIF-76-10%-25%	69.29	0.058	0.33, 0.63, 0.82
aZIF-76-20%-25%	75.16	0.063	0.33, 0.63, 0.82
aZIF-76-40%-25%	90.35	0.076	0.33, 0.63, 0.82
aZIF-76-60%-25%	88.52	0.075	0.33, 0.63, 0.82

Tab. S4 Mesopore porosity analysis for aZIF-76-40%-y.

Samples	[a]S_{BET} (m^2/g)	[b]V_{meso}/[c]V_{micro}	[d]D_{NLDFT} (nm)
aZIF-76-40%-5%	191.24	1.08	1.5~6.3
aZIF-76-40%-15%	284.00	1.05	1.5~15.0
aZIF-76-40%-25%	338.28	0.97	1.5~19.9

Tab. S5 Micropore porosity analysis for aZIF-76-40%-y.

Samples	[a]S_{BET} (m^2/g)	[b]V_{micro} (cm^3/g)	[c]D_{NLDFT} (nm)
aZIF-76-40%-5%	48.66	0.043	0.33, 0.63, 0.82
aZIF-76-40%-15%	59.53	0.052	0.33, 0.63, 0.82
aZIF-76-40%-25%	90.35	0.076	0.33, 0.63, 0.82

References

1 C. Zhou, L. Longley, A. Krajnc, G. J. Smales, A. Qiao, I. Erucar, C. M. Doherty, A. W. Thornton, A. J. Hill and C.W., *Nat. Commun.*, 2018, **9**, 5042.

2 B. Ravel and M. Newville, ATHENA, ARTEMIS, HEPHAESTUS: data analysis for X-ray absorption spectroscopy using IFEFFIT, *Journal of Synchrotron Radiation*, 2005, **12**, 537–541.

3 S. I. Zabinsky, J. J. Rehr, A. Ankudinov, R. C. Albers, M. J. Eller, Multiple-Scattering Calculations of X-ray-Absorption Spectra, *Phys. Rev. B*, 1995, **52**, 2995−3009.